Investigation of Self-Healing Behaviour in Cemented Paste Backfill

Weizhou Quan[1] and Mamadou Fall[2]

[1]University of Ottawa, Ottawa, ON, Canada, wquan091@uottawa.ca
[2]University of Ottawa, Ottawa, ON, Canada, mfall@uottawa.ca

Abstract

The presence of cracks within the cemented paste backfill (CPB) matrix can stem from multiple factors, such as excessive pressures from CPB overburden, stresses induced by the closure of adjacent rock walls, rockbursts, and shrinkage. These cracks significantly compromise structural integrity and mechanical strength while increasing permeability and impacting safety, durability, and environmental performance. While the self-healing technique has been extensively explored to repair cracks and reduce maintenance costs in conventional cementitious materials (eg, concrete, mortar), limited studies have delved into CPB's self-healing capability. This study aims to explore the self-healing (autogenous healing) behavior within CPB materials, evaluating the healing efficiency in restoring mechanical strength and hydraulic conductivity.

CPB samples were pre-cracked at different levels of pre-cracking to initiate a variety of crack widths after initial curing. Subsequently, these samples underwent self-healing periods ranging from 7–90 days. The results revealed a significant self-healing capacity within CPB materials. After 7 days of self-healing, pre-cracked specimens restored mechanical and permeation properties to levels comparable to uncracked control specimens without external intervention. Moreover, CPB specimens with high pre-cracking levels even exhibited up to a 22% increase in mechanical strength compared to control specimens after a 90 day self-healing period. This suggests that cracks within the CPB matrix can enhance hydration reactions, thereby favoring improved self-healing performance. These findings provide valuable insights into CPB's self-healing behaviour, holding significant implications for engineering CPB structures, evaluating their safety, durability, and serviceability, and offering sustainable solutions for the mining industry.

Key words: tailings, cemented paste backfill, self-healing, cracks, mechanical property, hydraulic conductivity

Introduction

CPB stands as an integral solution in modern mining practices by enhancing productivity, managing waste efficiently, and bolstering safety, while aligning with sustainability goals. This engineered, cementitious mixture comprises tailings with a solid percentage of 70–85%, binders with typically 3–7%, and water, all of which play a crucial role underground in providing ground support, facilitating waste disposal, and ensuring a secure working environment. However, cracks can develop in CPB materials or structures mirroring a common issue observed in traditional cementitious materials such as concrete and mortar. The formation of these cracks can be attributed to various processes or factors, including excessive stresses from the pressure of CPB overburden, stresses induced by the closure of rock walls adjacent to or surrounding CPB structures, as well as rock burst incidents and shrinkage. The existence of cracks in CPBs has a detrimental impact, weakening the structural integrity and mechanical strength while also elevating permeability properties. Consequently, this compromises safety, serviceability, durability, and environmental performance. These vulnerabilities are a cause for concern, particularly in the context of deep mining where heightened stresses from rock wall closure and increased intensity and frequency of rock bursts prevail. Furthermore, CPB structures can extend from a few tens to several hundred meters underground in at least one dimension, rendering manual maintenance and crack repair impractical in real-world scenarios, and making it necessary to explore the self-healing capability of CPB.

It is well acknowledged that cementitious materials possess the potential for self-healing (De Belie et al., 2018; Ferrara et al., 2017; Li and Herbert, 2012; Roig-Flores et al., 2016). Natural self-healing involves

the automatic repair of cracks in cementitious materials, an ability rooted in their inherent self-healing potential. This type of self-healing (autogenous healing) involves the inherent ability of the material to repair cracks through chemical, physical, and mechanical mechanisms within the matrix itself (Cuenca and Ferrara, 2017). Chemical mechanisms involve the hydration of unhydrated cement particles and subsequent carbonation of calcium hydroxide ($Ca(OH)_2$) to generate calcite ($CaCO_3$) which fills cracks (Edvardsen, 1999; Ramm and Biscoping, 1998). Additionally, the physical swelling of calcium silicate hydrates and the mechanical action of loose particles also contribute to autogenous healing (De Belie et al., 2018). In typical conventional concrete with a water-to-cement ratio ranging from 0.4–0.55, around 30% of cement particles remain unhydrated during initial curing time. Upon exposure to moisture or water penetrating through cracks, these dormant cement particles resume hydration, producing delayed hydration products to mend the cracks and restore material integrity. This self-healing capability not only minimizes cost requirements but also efficiently maintains or restores cracked cementitious infrastructures. By automatically addressing cracks, the embedded self-healing systems within these structures helps mitigate permeability, rejuvenate structural functionality, enhance durability, and dramatically extend their service life.

Despite the importance of self-healing processes and their prevalence in conventional concrete materials, there is a lack of research on the self-healing capabilities and behaviour of CPB, along with its influence on the restoration of mechanical and permeation properties. Additionally, the variation in cement content and water content in CPBs, as well as differences in particle size distributions (ie, between tailings in CPB and aggregates in concrete) highlights the inapplicability of findings from self-healing studies on conventional concrete and cement-based materials to CPB materials. Addressing this gap in knowledge and technology is imperative. As such, this paper aims to explore CPB's self-healing behaviour and assess its efficacy in restoring mechanical and permeation properties, thereby laying a foundation for understanding and ablity with which to harness this phenomenon in CPB materials.

Materials and Methods

Materials

Silica tailings (ST), composed primarily of 99.8% quartz SiO_2 and prevalent in Canadian hard rock mines, were employed in this study. The aim was to precisely regulate the chemical and mineral components of the tailings to ensure minimal uncertainties when examining the sole influence of combined components of CPB. Analysis revealed that the grain size distribution of ST closely resembled the average of nine natural tailings (NT) from Canadian mines. Portland Cement Type I (PCI) served as the binder, and tap water was used to prepare the CPB mixtures.

Sample preparation and initial crack introduction

The primary goal of this study is to explore the self-healing capability of the CPB matrix. For this purpose, specimens measuring Φ50 × 100 mm were cast, employing a binder PCI ratio of 4.5% and a constant water-to-cement ratio (w/c) of 7.35 by weight. These specimens underwent curing under room conditions with initial curing (IC) periods of 7 days (IC7) before crack initiation. Subsequent to the initial curing period, the studied specimens were subjected to specific pre-cracking levels (Figure 1), namely 0, 30, 50, 75, or 90%, referred to as control, PC-30, PC-50, PC-75, or PC-90%, respectively, and relative to results of uniaxial compressive strength (UCS) tests. These tests induced varying levels of crack damage within the specimens. Upon reaching the predetermined pre-load values, the applied load was sustained for one minute before being released, and the pre-cracked specimens were then prepared for the self-healing process.

Healing conditions

Following the introduction of initial cracks, the pre-cracked specimens were enveloped in plastic films and stored under room conditions for self-healing curing. This specific curing setup, devoid of external

interference, aimed to examine the inherent self-healing potential of the CPB material. The uncracked control specimens were cured under the same conditions as the studied specimens, allowing for comparative analysis.

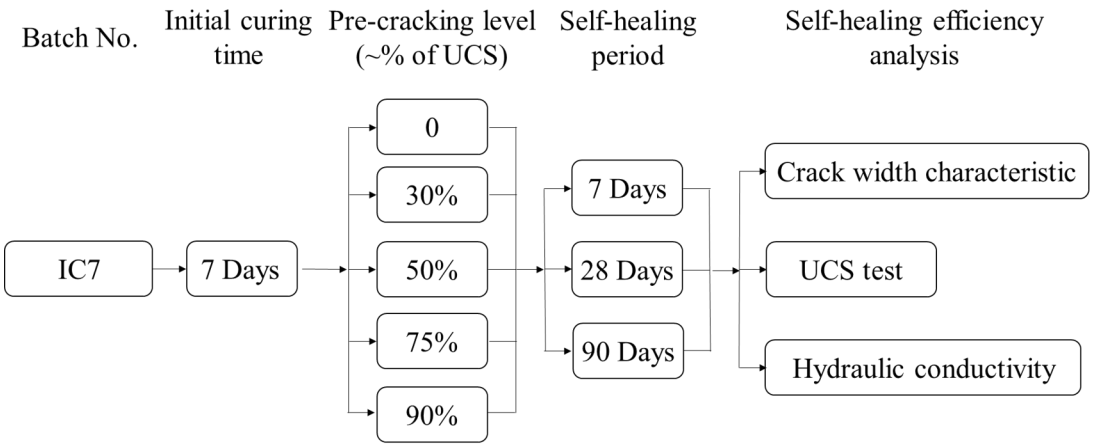

Figure 1. Overview of the experimental design.

Self-healing examination

Crack observance

A digital microscope capable of 200 × magnification and integrated with computer software was employed as an additional technique to monitor changes in crack width. This allowed directly assessment of the self-healing performance of pre-cracked specimens following exposure to healing conditions. Initial crack width measurements were taken from multiple positions on each crack immediately after their introduction. Subsequent measurements were carried out at intervals of 7, 28, and 90 days during the self-healing process.

Hydraulic conductivity monitoring

Saturated hydraulic conductivity (k_{sat}) tests were performed using a triaxial cell with a flexible wall technique in accordance with ASTM 5084-16a to assess the changes in hydraulic conductivity of pre-cracked and healed CPB specimens. The test involved employing a constant head method, wherein a consistent hydraulic gradient (10 psi or 69 kPa) between the inflow and outflow was maintained for measurement purposes.

The hydraulic conductivity recovery ratio (HCRR) in this study was determined as:

$$\mathrm{HCRR}\ (\%) = \frac{k_0 - k_{ah}}{k_0} \qquad \text{Equation 1}$$

where k_0 is the initial hydraulic conductivity, cm/s, measured after pre-cracking process; k_{ah} is the hydraulic conductivity, cm/s, measured after self-healing period.

Strength recovery monitoring

The compression test can serve as an approach to assess the mechanical strength restoration of CPB specimens through a self-healing process. Therefore, UCS tests were conducted on at least three CPB specimens to gauge the strength recovery in CPB materials, following ASTM C39/C39M-21 standard. The tests were performed at intervals of 7, 28, and 90 days during the self-healing process on both healed pre-cracked specimens and uncracked control specimens.

The calculation for the percentage decrease in UCS after the initiation of pre-cracks is determined by:

$$S_{d\%} = \frac{S_0 - S_{pc}}{S_0} \quad \text{Equation 2}$$

where $S_{d\%}$ is the percentage of UCS decrease, S_0 is the initial compressive strength of uncracked control specimens, and S_{pc} is the compressive strength of pre-cracked specimens before healing.

Subsequent to self-healing periods, the relative changes in compressive strength (CCS) of the healed specimens compared to control specimens can be calculated by:

$$\mathrm{CCS}\ (\%) = \frac{S_{ah} - S_{control}}{S_{control}} \quad \text{Equation 3}$$

where S_{ah} represents the compressive strength of the healed pre-cracked specimens, and $S_{control}$ denotes the compressive strength of uncracked control specimens.

Porosity and void ratio determination

The mechanical properties of CPB materials are typically influenced by their physical properties, such as void ratio, porosity, and water content (Ghirian and Fall, 2013). Throughout the self-healing periods, the alterations in void ratio and porosity of the healed pre-cracked specimens were examined. This investigation aimed to gain insights into the microstructural modifications induced by the self-healing behavior within the CPB matrix.

Characterization of self-healing materials

A range of microstructural techniques, including X-ray diffraction (XRD), scanning electron microscopy-energy dispersive spectroscopy (SEM-EDS), and thermogravimetric analysis (TGA), were employed to delve into the constituents of self-healing materials inside the cracks. SEM-EDS analysis focused on the surfaces of cracks to observe the microstructure and identify the primary chemical elements present in the self-healing materials. In addition, samples of self-healing materials obtained from the healed cracks were collected for XRD analysis to delineate the chemical components present in the cracks. TGA analysis involved the preparation of powders from both control specimens and healed pre-cracked specimens to track differences in the extent of cement hydration between each sample type with the influence of the pre-cracking process.

Representative Experimental Results and Discussions

Crack characteristics

Multiple levels of pre-cracking were applied to introduce microcracks on the studied specimens during the initial pre-cracking process. Notably, the microcracks were hardly generated at the pre-cracking levels of PC-30% and PC-50%. These levels, up to 50% of final UCS, exhibited elastic behavior (Fall et al., 2007). However, as the pre-cracking load approached the peak region (PC-75% and PC-90%), the behavior transitioned into the first non-linear phase, and microcracks started to appear on the CPB specimens. The progressive increase in load facilitated the crack propagations until reaching the peak stress. Consequently, discernible cracks on the pre-cracked specimens became more apparent as the pre-cracking levels increased.

The microcracks examined before and after self-healing exhibited three distinct healing scenarios, including: complete healing (Figure 2), partial healing (Figure 3), and no healing. The partially or completely healed microcracks were characterized by the presence of white crystal-like substances that

filled the cracks after specific self-healing intervals. This study identified the maximum crack widths that could be healed under varying self-healing periods, serving as indicators of the CPB material's autogenous healing capability (Table 1). Remarkably, cracks exhibited increased healing widths with extended self-healing periods. It was noticed that Batch IC7 displayed superior autogenous healing within the first 7 days of the self-healing period, possibly attributed to a higher content of unhydrated cement particles during the early curing stage. This proposition on the efficiency of autogenous healing in pre-cracked specimens was substantiated by TGA analysis. Pre-cracked specimens at the early self-healing period (D0) performed lower curves associated with weight loss and phase transformations (see Figure 6); this indicated a lower hydration level and higher content of unhydrated cement during the early self-healing period, thus leading to more effective closure of surface cracks. Moreover, Figure 3 demonstrated diminished self-healing efficacy with larger crack widths. Partially healed cracks depicted the development and growth of healing products from both sides of the crack towards the center, aiming to bridge the gap. This partial healing process underscored the inherent limitation of the CPB matrix in autogenous healing, marking a threshold in crack closure. Consequently, crack width significantly impacts the self-healing efficiency of CPB materials, aligning with similar findings in other cementitious materials (Huang et al., 2016; Jiang et al., 2015; Maes et al., 2014). Narrower and shallower cracks exhibit a higher potential for complete healing due to their smaller volume requiring repair.

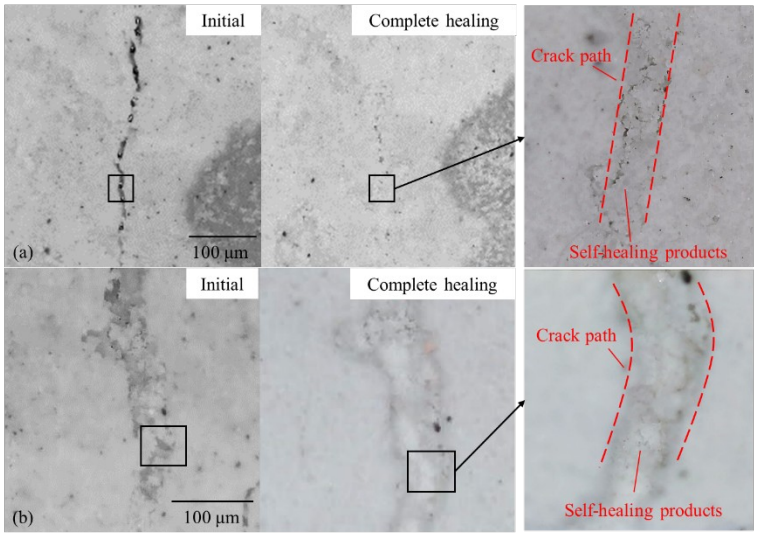

Figure 2. Typical observation of complete healing.

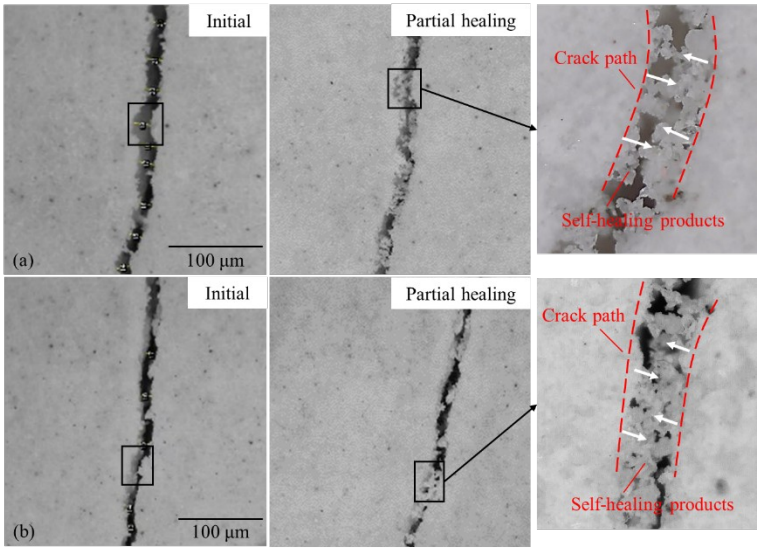

Figure 3. Typical observation of partial healing in large cracks

Table 1. Maximum crack width healed after self-healing periods.

Batch	Self-healing period (Day)	Maximum healed crack width (μm)
IC7	7	46.1
	28	56.1
	90	67.9

Self-healing materials

As aforementioned, the completely healed microcracks exhibited filling with white crystal-like substances. Understanding the underlying mechanisms governing this observed self-healing behavior necessitates characterizing the chemical/mineralogical composition of the self-healing materials within the CPB matrix.

XRD analysis was performed on powder-phase self-healing materials collected from the healed cracks. Figure 4 illustrates the XRD patterns of both self-healing materials and CPB materials from control specimens. It is found that a substantial difference in peaks, primarily related to calcite (CC) among $Ca(OH)_2$ (CH), C-S-H, C_3S, and C_2S, was observed within the two-theta range of 30–65°. These differences suggest a higher abundance and intensity of CC in self-healing products compared to regular CPB materials, suggesting CC as the principal self-healing product within CPB cracks. Additionally, SEM-EDS analysis was conducted on a healed crack surface to visualize the microstructure of self-healing materials and identify their chemical compositions. Figure 5 showcases representative SEM-EDS micrographs from various analyzed locations. The EDS diagrams clearly detected traces of Ca, Al, C, and O peaks, suggesting the presence of a combination of C-S-H, $Ca(OH)_2$, and $CaCO_3$ as the primary self-healing materials within CPB cracks. However, these detected products might be influenced by adjacent phases bleeding into each other due to limitations of EDS (Kan et al., 2010), and the application of epoxy during sample preparation may have disrupted the substances within the cracks. Furthermore, TGA analysis conducted on powders collected from both control and pre-cracked specimens unveiled a higher level of cement hydration and $Ca(OH)_2$ carbonation in the pre-cracked specimens after identical self-healing periods. Figure 6 depicts the notably higher weight loss in pre-cracked specimens at temperatures of 600–800°C which suggests $CaCO_3$ decomposition, and at temperatures of 110–200°C which suggests

C-S-H dehydration. These TGA results align with findings from XRD and SEM-EDS analyses and provide substantial evidence that the primary self-healing products within CPBs consist of a combination of C-S-H, $Ca(OH)_2$, and $CaCO_3$. Consistency among all microstructure analysis techniques supports this conclusion.

Recovery of compressive strength

The development of compressive strength in the control and self-healing specimens is depicted in Figure 7, where those subjected to PC-30% and PC-50% levels exhibited higher UCS values compared to the control specimens immediately after the pre-cracking process (at Day 0). For instance, CPB specimens subjected to PC-50% display up to a 37.5% strength increase over the control specimens. This augmented strength in CPB is attributed to the CPB material's volume contraction behavior under uniaxial compressive loading (Fall et al., 2009). As aforementioned, these CPB specimens, compacted under these two pre-cracking levels without observed cracks, resulted in denser and less porous material, known to correlate with higher strength (Fall et al., 2009; Ghirian & Fall, 2015). Conversely, CPB samples with higher pre-cracking levels exhibit decreased strengths compared to control samples at Day 0. For example, a pre-cracking level of PC-75% resulted in a 14.3% reduction in strength. Furthermore, a decline of 22.0% in compressive strength was observed for specimens pre-cracked at PC-90%. This decline in strength among pre-cracked CPB specimens at levels of PC-75% or higher, and the subsequent decrease as the pre-cracking level increases from PC-75% to PC-90%, is primarily due to crack generation and propagation within the CPB specimens. The formation of these cracks intensifies with higher pre-cracking levels.

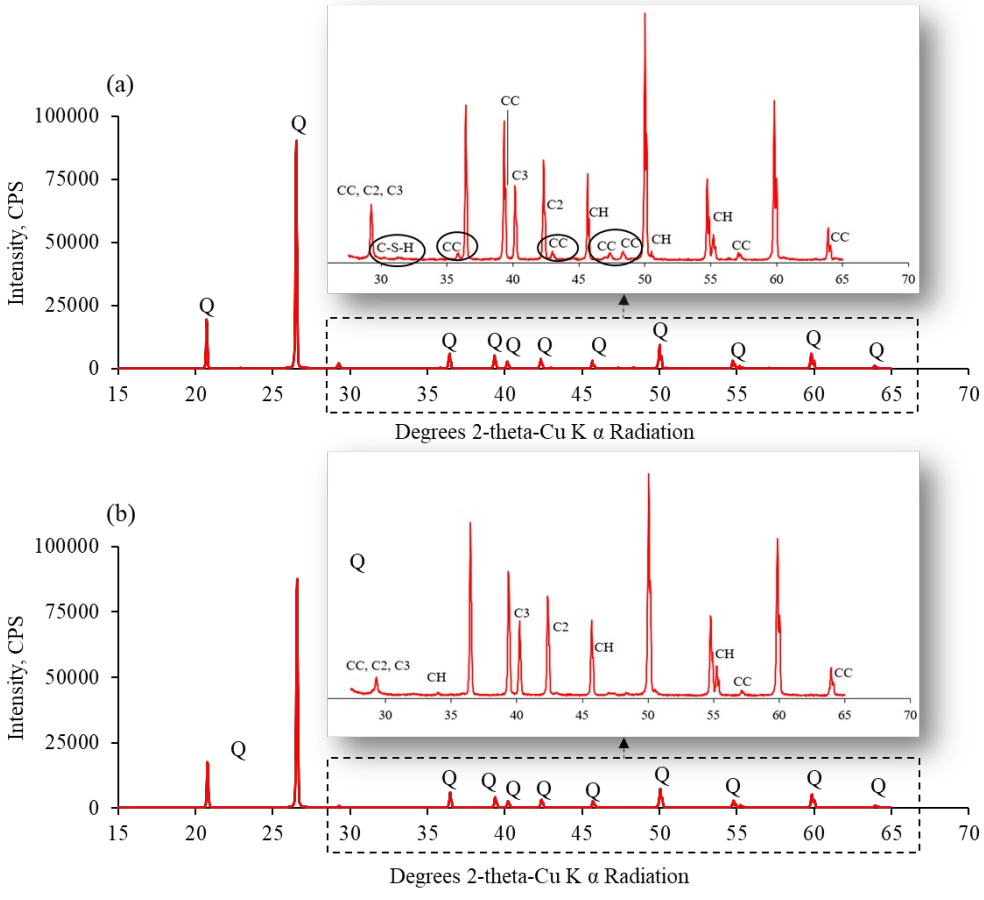

Figure 4. XRD patterns of (a) surface self-healing materials and (b) control CPB specimen.

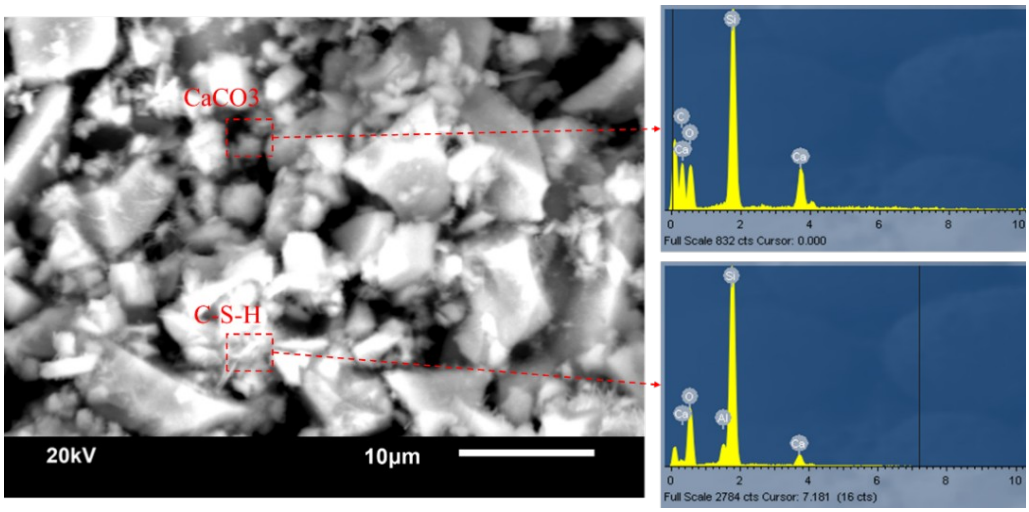

Figure 5. SEM images of the crack surface (left) and EDS patterns (right) of detected self-healed materials.

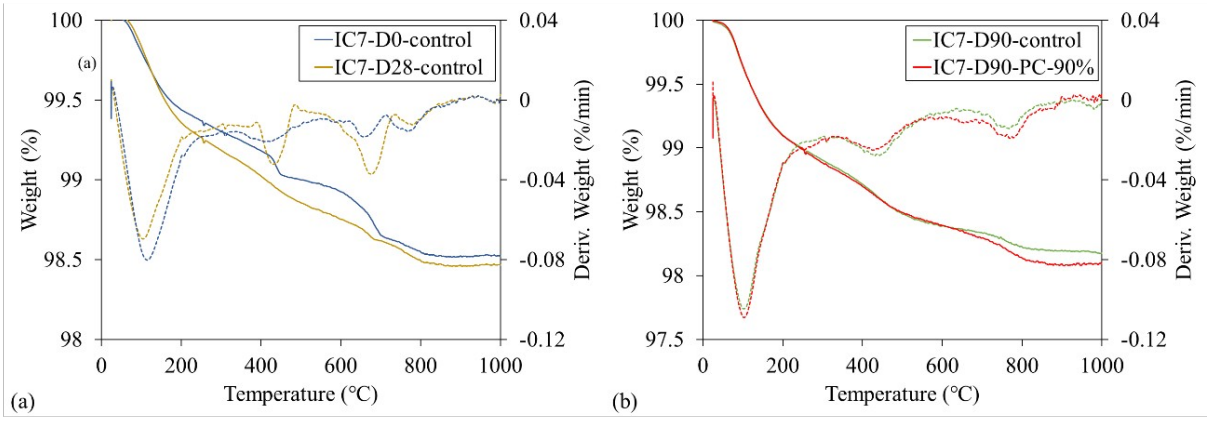

Figure 6. TG/DTG analysis of (a) control specimens at the curing periods of D7 and D28 and (b) pre-cracking impact on cement hydration

After 7 days of self-healing (Day 7), the compaction effect induced by mechanical pre-loads PC-30% and PC-50% diminishes (Figure 7), exhibiting strengths almost equivalent to control samples. Moreover, pre-cracked specimens of PC-75% and PC-90% also recover compressive strength values similar to those of control specimens. With prolonged self-healing, these pre-cracked specimens of PC-75% and PC-90% gradually achieve even higher compressive strengths than control specimens. For example, the specimens with a PC-75% pre-cracking level restored strengths 7.1% higher than control specimens after 28 days of self-healing (Day 28). Furthermore, this increase is more pronounced in specimens with a higher pre-cracking level of PC-90% and an extended self-healing period (Day 90) with an increase of up to 22%, suggesting that pre-cracks within the CPB matrix might enhance the hydration reactions. As demonstrated in Figure 6b, a higher weight loss of CaCO3 in PC-90% specimen between 600–800℃ was observed compared to control specimens; this means a higher $Ca(OH)_2$ carbonation occurred in pre-cracked CPB specimens after the 90 day self-healing period. The additional CaCO3 produced further favours crack closure and strength restoration. Overall, this enhanced strength recovery is attributed to autogenous

healing within the CPB material, wherein continuous cement hydration governs the mechanical strength recovery and development in the studied CPB specimens. The generation of microcracks allows the penetration of the essential elements (O_2, CO_2, and H_2O) into the CPB matrix, accelerating cement hydration and $Ca(OH)_2$ carbonation (Ghirian and Fall, 2015; Huang et al., 2016; Song et al., 2006). As self-healing progresses, hydration products fill the voids and cracks to reduce the porosity, which refines the pore structures within the CPB matrix and contributes to mechanical strength restoration (Fall et al., 2009).

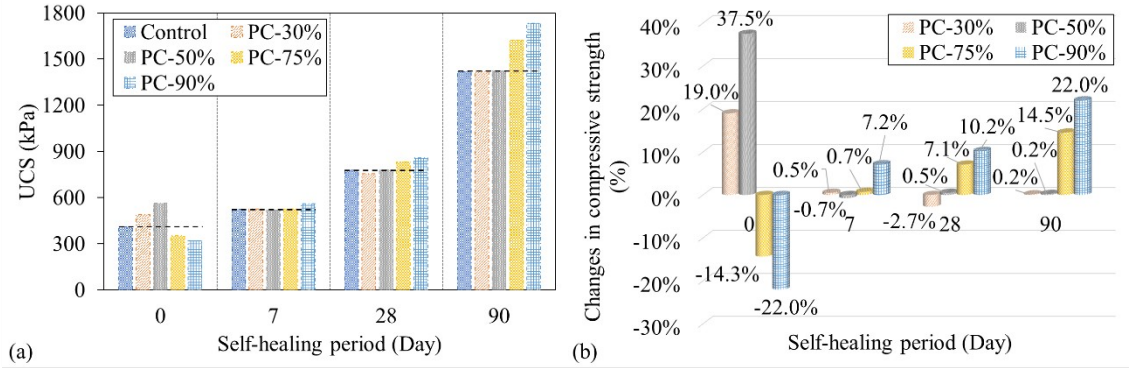

Figure 7. Plots of: a) compressive strength development, and b) changes in compressive strength (CCS) in pre-cracked specimens with different self-healing periods.

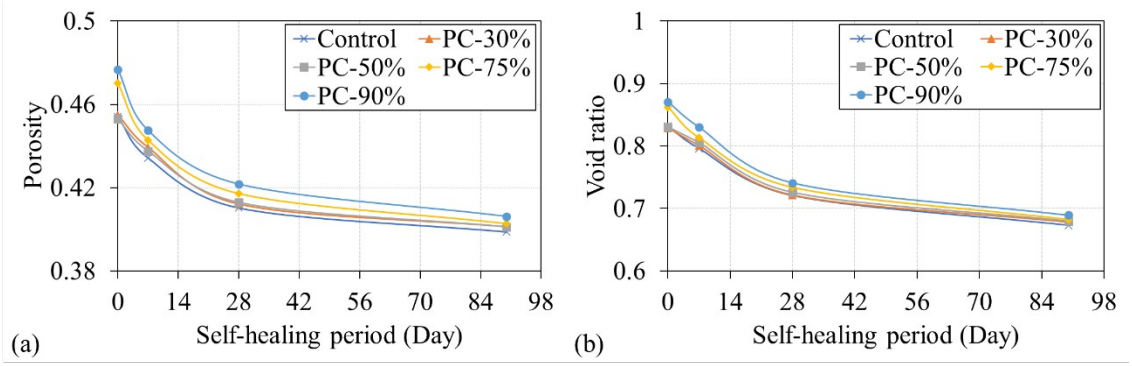

Figure 8. Changes in: a) porosity, and b) void ratio of pre-cracked specimens over self-healing periods.

Recovery of hydraulic conductivity

Figure 9 depicts the evolution of saturated hydraulic conductivity (k_{sat}) in different pre-cracked CPB specimens across various self-healing periods, providing insight into CPB self-healing behavior through permeability performance. Initial pre-cracking levels (PC-30% and PC-50%) impacted hydraulic conductivity minimally compared to control specimens immediately after the pre-cracking process (Day 0). This was attributed to CPB's volumetric contraction under compressive loading, resulting in rare crack generation at these levels (Fall et al., 2009). However, beyond the threshold stress (PC-75% and PC-90%), k_{sat} values sharply increased because of macrocrack formation, compromising the pore structure and allowing rapid water flow.

Throughout the self-healing process, Figure 9 illustrates a progressive decrease in k_{sat} values. This decline is associated with autogenous healing involving continuous cement hydration and $Ca(OH)_2$ carbonation, and leading to the formation of self-healing materials that modify the CPB's pore structure. As self-healing continued, these self-healing materials filled voids and cracks, refining the pore structure and

blocking internal connections which resulted in decreased k_{sat} values. This trend aligns with the observed decreasing porosity and void ratio as self-healing progressed (Figure 8). Additionally, TGA results (Figure 6) confirm that higher cement hydration levels occurred in specimens with high pre-cracking levels, where cracks facilitated CO_2, O_2, and H_2O flow, expediting carbonation and cement hydration to produce more self-healing products. Notably, after 90 days of self-healing, specimens at PC-75% achieved k_{sat} values similar to control specimens. The calculated hydraulic conductivity recovery ratios (HCRR) for the highest pre-cracked specimens (PC-90%) reached 86.9%, indicating the occurrence of robust autogenous healing within the CPB matrix. This healing process generated sufficient self-healing materials to achieve hydraulic conductivities, porosities, and void ratios similar to those of control specimens.

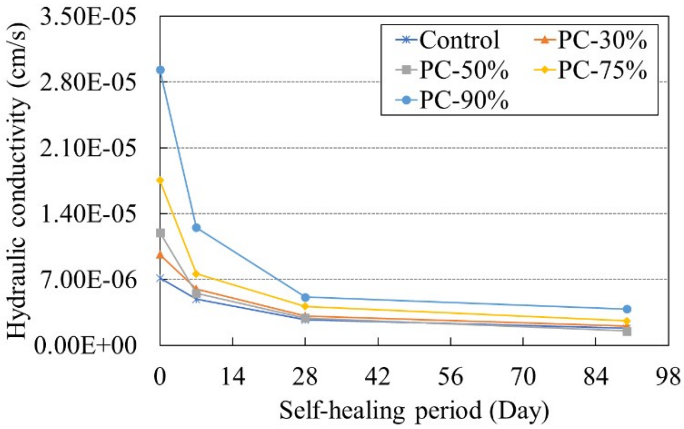

Figure 9. Changes of hydraulic conductivity with varying pre-cracking levels and self-healing periods

Conclusions

This paper presents the experimental findings from a study focused on the evaluation of the self-healing behaviour in CPB material and the assessment of the efficiency of self-healing materials. The results reveal that CPB materials have a robust inherent capacity for self-healing. Microcracks in CPB material exhibit self-healing under ambient exposure conditions without external intervention. Notably, the maximum crack width of 67.9 μm can be completely healed after a self-healing period of 90 days in this study. However, the presence of partially healed and non-healed cracks highlights the limitation in the self-healing for the studied CPB material.

Additionally, it is demonstrated that the combination of $CaCO_3$, $Ca(OH)_2$, and C-S-H is most likely to be the primary self-healing materials in the CPB matrix. The calcite $CaCO_3$ is the main substance of the white crystal-like self-healing material formed inside the cracks. Furthermore, the pre-cracked CPB specimens exhibit recovery to strengths comparable to uncracked control specimens after only 7 days of the self-healing period. In the extended self-healing periods, the CPB specimens with high pre-cracking levels (PC-75% and PC-90%) demonstrated up to a 22% increase in strength compared to control specimens after a 90 day self-healing period. Moreover, achieving a hydraulic conductivity recovery ratio of 86.9% in PC-90% pre-cracked specimens suggests that pre-existing cracks stimulate the formation of self-healing materials, filling the cracks to restore and enhance the self-healing capability.

References

Cuenca, E., & Ferrara, L. (2017) Self-healing capacity of fiber reinforced cementitious composites. State of the art and perspectives. KSCE Journal of Civil Engineering, 21, 2777-2789. https://doi.org/10.1007/s12205-017-0939-5

De Belie, N., Gruyaert, E., Al-Tabbaa, A., Antonaci, P., Baera, C., Bajare, D., . . . Jefferson, T. (2018) A review of self-healing concrete for damage management of structures. Advanced materials interfaces, 5(17), 1800074. https://doi.org/10.1002/admi.201800074

Edvardsen, C. (1999) Water permeability and autogenous healing of cracks in concrete. In Innovation in concrete structures: Design and construction (pp. 473-487): Thomas Telford Publishing.

Fall, M., Adrien, D., Célestin, J. C., Pokharel, M., & Touré, M. (2009) Saturated hydraulic conductivity of cemented paste backfill. Minerals Engineering, 22(15), 1307-1317. https://doi.org/10.1016/j.mineng.2009.08.002

Fall, M., Belem, T., Samb, S., & Benzaazoua, M. (2007) Experimental characterization of the stress–strain behaviour of cemented paste backfill in compression. Journal of Materials Science, 42(11), 3914-3922. https://doi.org/10.1007/s10853-006-0403-2

Ferrara, L., Krelani, V., Moretti, F., Flores, M. R., & Ros, P. S. (2017) Effects of autogenous healing on the recovery of mechanical performance of High Performance Fibre Reinforced Cementitious Composites (HPFRCCs): Part 1. Cement and concrete composites, 83, 76-100. https://doi.org/10.1016/j.cemconcomp.2017.07.010

Ghirian, A., & Fall, M. (2013) Coupled thermo-hydro-mechanical–chemical behaviour of cemented paste backfill in column experiments. Part I: Physical, hydraulic and thermal processes and characteristics. Engineering Geology, 164, 195-207. https://doi.org/10.1016/j.enggeo.2013.01.015

Ghirian, A., & Fall, M. (2015) Coupled Behavior of Cemented Paste Backfill at Early Ages. Geotechnical and Geological Engineering, 33(5), 1141-1166. https://doi.org/10.1007/s10706-015-9892-6

Huang, H., Ye, G., Qian, C., & Schlangen, E. (2016) Self-healing in cementitious materials: Materials, methods and service conditions. Materials & Design, 92, 499-511. https://doi.org/10.1016/j.matdes.2015.12.091

Jiang, Z., Li, W., & Yuan, Z. (2015) Influence of mineral additives and environmental conditions on the self-healing capabilities of cementitious materials. Cement and concrete composites, 57, 116-127. https://doi.org/10.1016/j.cemconcomp.2014.11.014

Kan, L.-L., Shi, H.-S., Sakulich, A. R., & Li, V. C. (2010) Self-Healing Characterization of Engineered Cementitious Composite Materials. ACI Materials Journal, 107(6), 617-624. Retrieved from https://qe2a-proxy.mun.ca/login?url?url=https://www.proquest.com/scholarly-journals/self-healing-characterization-engineered/docview/811255249/se-2?accountid=12378

Li, V. C., & Herbert, E. (2012) Robust self-healing concrete for sustainable infrastructure. Journal of Advanced Concrete Technology, 10(6), 207-218. https://doi.org/10.3151/jact.10.207

Maes, M., Van Tittelboom, K., & De Belie, N. (2014) The efficiency of self-healing cementitious materials by means of encapsulated polyurethane in chloride containing environments. Construction and Building Materials, 71, 528-537. https://doi.org/10.1016/j.conbuildmat.2014.08.053

Ramm, W., & Biscoping, M. (1998) Autogenous healing and reinforcement corrosion of water-penetrated separation cracks in reinforced concrete. Nuclear Engineering and Design, 179(2), 191-200. https://doi.org/10.1016/S0029-5493(97)00266-5

Roig-Flores, M., Pirritano, F., Serna, P., & Ferrara, L. (2016) Effect of crystalline admixtures on the self-healing capability of early-age concrete studied by means of permeability and crack closing tests. Construction and Building Materials, 114, 447-457. https://doi.org/10.1016/j.conbuildmat.2016.03.196

Song, H.-W., Kwon, S.-J., Byun, K.-J., & Park, C.-K. (2006) Predicting carbonation in early-aged cracked concrete. Cement and Concrete Research, 36(5), 979-989. https://doi.org/10.1016/j.cemconres.2005.12.019